

Calculation of the vibration properties of the Pd/Au (111) ordered surface alloy in its stable domain

R. Chadli^{1,2,a}, A. Khater¹, and R. Tigrine²

¹LPEC, Université du Maine, Av. Olivier Messiaen, 72085 Le Mans Cedex 09, France

²LPCQ, Université Mouloud Mammeri, B.P. N° 17, 15000 Tizi-Ouzou, Algérie

Abstract. In the present paper, a calculation is presented for the vibration properties of the ordered surface alloy $\text{Au}(111) - (\sqrt{3} \times \sqrt{3})\text{R}30^\circ - \text{Pd}$, which is a stable system in the temperature range of 500K to 600K. This surface alloy is formed by depositing Pd atoms onto the Au(111) surface, and annealing at higher temperatures. The matching theory is applied to calculate the surface phonons and local vibration densities of states (LDOS) for the clean Au (111) surface, and for the $\text{Au}(111) - (\sqrt{3} \times \sqrt{3})\text{R}30^\circ - \text{Pd}$ surface alloy. Our theoretical results for the surface phonon branches of the clean Au (111) surface compare favorably with previous *ab initio* results and experimental data. In contrast, there are no previous results for the vibrational LDOS for the atomic Au site in a clean Au (111) surface, or results for the surface phonons and vibration spectra for the surface alloy. The surface phonons are calculated for the clean Au (111) surface and the ordered surface alloy along three directions of high symmetry, namely $\overline{\Gamma\text{M}}$, $\overline{\text{MK}}$, and $\overline{\text{K}\Gamma}$. The phonon branches are strongly modified from the Au (111) surface to the surface alloy. In particular a remarkable change takes place for the LDOS between the clean Au (111) surface and the surface alloy, which may find its origin in the charge transfer from Au atoms to Pd atoms.

1 Introduction

Many physical and chemical processes of technical importance take place at solid surfaces, such as catalysis and corrosion. The best understanding of these processes on a nanometric scale requires a proper knowledge of structural, electronic, and dynamical properties of the substrate surface. The crystal surface provokes large modifications in the inter-atomic binding in the first few atomic layers, and this has a significant influence on the surface properties compared to those in the bulk. The vibration properties of atoms in the surface atomic layers are important to study because surface phenomena like adsorption, diffusion or growth can be significantly influenced by the vibration dynamics of these surface layers. The study of the lattice dynamics of surfaces, helps, furthermore, to characterize the surface properties, and is complementary to other investigations of the surface structural and electronic properties [1].

^ae-mail : rabah_abo@yahoo.fr

It is now well established that the deposition of a reactive metal upon a noble metal surface substrate often creates a surface alloy, which has physical and chemical properties that are different from those of the surfaces of the component metals. This method for creating surface alloys is used to make metallic surfaces for specific use in numerous applications, including heterogeneous catalysis, where the electronic structure and geometric arrangement of the surface atoms strongly influence the reaction. Thus a refined understanding of the physical and chemical properties of surface alloys appears to be essential in order to make further progress in the control of catalytic effects [2, 3].

One of the most important metals for industrial applications, and also for fundamental studies, is palladium because of its high catalytic activity towards many chemical reactions (in vacuum and in solution), and its ability to absorb hydrogen [4-7]. Recently, a great deal of attention has been focused on the physics and chemistry of palladium deposited on different metal surfaces in the form of bimetallic surfaces, owing to the significant differences in the electronic and chemical properties of Pd at surfaces from Pd in the bulk [8-10]. Among such bimetallic systems, Pd-Au has received considerable attention because of its use for a number of catalytic reactions, as for example CO oxidation, cyclotrimerization of acetylene, synthesis of vinyl acetate monomer, selective oxidation, and many other applications such as hydrogen fuel cells and pollution control systems [11-14].

Furthermore, there are situations when the Pd alloys itself to Au. The first studies of Pd-Au alloys have addressed primarily two types of model systems: stable bulk alloys, and stable surface alloys prepared by the deposition of one metal on a selected surface of a single crystal of the other. An example is the deposition of Pd metal on the Au (111) surface [15-17], and of Au metal on the Pd(111) surface [18].

The surfaces (111) of noble metals, such as Au, Ag, and Cu, present electronic states called Shockley states localized on its surface [19-22]. For the Pd deposited on the Au(111) surface, the electronic states of a submonolayer of Pd < 1 ML have been studied using angle-resolved ultraviolet photoemission spectroscopy [23]. The Au(111) Shockley states persist, and a Pd state emerges. Both peaks due to the Au and Pd surface states shift to lower binding energies with increasing Pd coverage, whereas their half-widths are insensitive to the coverage. The observed spectral shifts are reported as caused by a charge transfer from the substrate to the deposited Pd.

Since the study of atomic vibrations and their interactions with electrons contributes to the understanding of the fundamental mechanisms for a variety of physical properties in crystals and at crystal surfaces, such as elastic, optic, and electrochemical properties, this has motivated the present work which is aimed at calculating the vibration dynamics of the ordered

Au(111) – ($\sqrt{3} \times \sqrt{3}$)R30° – Pd surface alloy.

The outline of this paper is as follows. In Sec. 2 we give a description of the ordered surface alloy structure and stability criteria. In Sec. 3 a brief description of the matching theory is presented and applied to calculate the localized surface phonons for the two types of surfaces, namely the reference clean Au(111) surface, and the ordered surface alloy **Au(111) – ($\sqrt{3} \times \sqrt{3}$)R30° – Pd**. The calculation of the local vibration density of states (LDOS) for the Au and Pd atoms in this surface alloy system is also presented. In Sec. 4, the different numerical results are discussed and interpreted, and conclusions are presented.

2 Description and stability of the **Au(111) – ($\sqrt{3} \times \sqrt{3}$)R30° – Pd** surface alloy

The two metals gold and palladium crystallize in a face-centered cubic structure with lattice parameters equal to 4.08 Å and 3.89 Å, respectively. Since Au and Pd are miscible in principle in the bulk, the occurrence of ordered surface structures may be expected [23]. The detailed morphology of Pd-Au systems varies strongly as a function of the preparation conditions in terms of deposition technique and annealing temperatures.

Pd ultrathin films on Au(111) surface substrate can be prepared by vapor deposition in ultrahigh vacuum (UHV), and studied over the substrate temperature range 150-650 K using different

methods, such as Auger electron spectroscopy (AES), low-energy ion-scattering spectroscopy (LEISS), X-ray photoelectron spectroscopy (XPS), and low-energy electron diffraction (LEED) [24-26]. Koel *et al.* have reported that the in-vacuum growth process of Pd atoms on Au(111) depends strongly on the substrate temperature [6, 27]. At a substrate temperature of 150 K, a pure Pd monolayer is formed on the Au(111) surface, as suggested by the evolution of AES signals. When the growth temperature is raised to 500 K, the LEIS data indicates the specific intermixing of Pd and Au [28, 29].

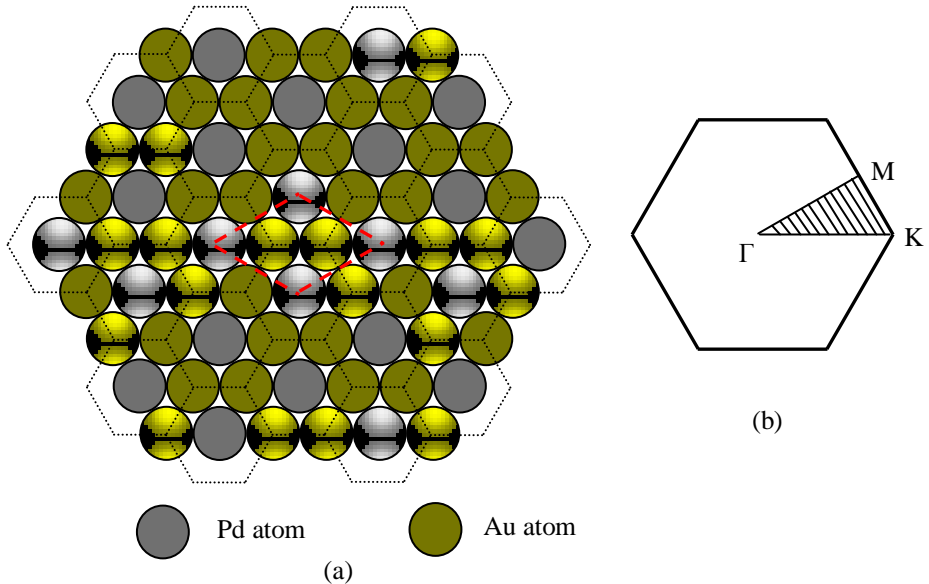


Fig.1. (a) A schematic representation for the $\text{Au}(111) - (\sqrt{3} \times \sqrt{3})R30^\circ - \text{Pd}$ ordered surface alloy, and the corresponding elementary unit cell. (b) First BZ of the corresponding reciprocal lattice, with the high-symmetry points indicated; the hatched area is the irreducible part.

The results given by Baddeley *et al.* [28], Chen *et al.* [30], and Atanasov *et al.* [23], show that for appropriate annealing temperatures of the gold substrate (≈ 500 K), an ordered surface alloy appears which exhibits $\sqrt{3}$ periodicity (see Figure 1 below). This surface alloy structure is stable in the temperature range [500K–600K] for a concentration equal to 1/3 ML of palladium atoms. The intermixed layer is composed of an Au rich alloy. The significant enrichment of Au at the first surface atomic layer is a consequence of surface free energy minimization, since this is 1.626 J/m^2 for Au which is lower than the corresponding value 2.043 J/m^2 for Pd. Furthermore, the spectroscopic properties of the Pd-induced electronic Shockley states indicate in reference [24], that these originate from the Au (111) surface states and are modified by the presence of monolayer Pd *islands* on the substrate. Since these experimental photoemission measurements are made at room temperature, for a submonolayer < 1 ML coverage of Pd, we conclude that it is probable that the ordered surface alloy may not be stable at room temperatures, leading to the reorganization of the Pd atoms in the form of islands on top of the Au surface. However, the question of the stability of this structure is not clear cut, and is not indicated in the different references cited for the surface alloy structure [23, 28, 30]. Although our results are general, we limit their validity here to the temperature range of [500K – 600K], where the stability of the $\text{Au}(111) - (\sqrt{3} \times \sqrt{3})R30^\circ - \text{Pd}$ surface alloy, although the question of this stability remains open for other temperature ranges.

3 Theoretical model for surface vibration dynamics

The surfaces of solid crystals destroy the three dimensional periodicity of the crystal. This leads to additional vibration modes at the surface absent in the bulk system. These modes are characterized by large displacements of atoms close to the surface and can be distinguished into two classes. The first class corresponds to surface localized modes whose frequencies are outside the bulk spectrum. These modes are well localized near the surface, and their amplitudes decay rapidly away from the surface into the bulk. The second class corresponds to the resonance modes, whose frequencies fall inside the bulk bands and thus deeply penetrate into the bulk [1].

The absence of translation symmetry in the direction perpendicular to the surface makes the Bloch theorem inapplicable along this direction. It becomes hence necessary to use an appropriate method for the analysis of the breakdown of periodicity. For the theoretical treatment of lattice dynamics at surfaces, different methods have been often used in the past, such as the Green's function method and the slab method. For the Green's function method, the surface is considered as a perturbation of the potential of the three dimensional crystal, and calculating the surface modes is formulated as a scattering problem via a Dyson equation [31]. This approach is especially useful to detect surface resonances, but is technically heavy. For the second approach, namely the slab method, the semi-infinite crystal is modeled numerically by a slab of finite thickness [32]. The thickness of the slab has to be large enough so that the two surfaces are decoupled dynamically. This ensures a proper representation of resonances deeply penetrating into the bulk.

In the present work, we use in particular the matching theory to investigate the vibration dynamics at the **Au(111) - ($\sqrt{3}x\sqrt{3}$)R30° - Pd** surface alloy. This method was initially used by Feuchtwang [33], and developed as a codified and theoretical tool by Szeftel and Khater [34]. It has since been further developed and applied extensively to study the propagation and scattering of phonons and magnons in crystalline solids and at surfaces and interfaces, in 1D, 2D and 3D nanostructures and low dimensional systems, [35-37]. The matching theory is called as such because its implementation requires the system under study to be divided into three regions all having the same periodicity along one sub domain of the system. For surface excitations these regions are namely a surface region, a bulk region, and an intermediate region which permits effectively the matching of surface states to bulk states.

The vibration dynamics of an atom in the bulk, located at the site ℓ may be described in the harmonic approximation with the following general equation of motion [38]

$$M_{Au} \omega^2 U_\alpha(\ell, \omega) = - \sum_{\ell'=\ell} \sum_{\beta} \frac{r_{\alpha\beta}}{r^2} K(\ell, \ell') [U_\beta(\ell', \omega) - U_\beta(\ell, \omega)] \quad (1)$$

The quantities (α, β) symbolize the three Cartesian directions $\{x, y, z\}$, M_{Au} the atomic mass of gold at sites ℓ given by $M_{Au} = 3.27 \times 10^{-25} \text{ kg}$, $U_\alpha(\ell, \omega)$ the displacement field along the α direction, r_α the corresponding Cartesian component of the radius vector between ℓ and ℓ' , where r is the distance between ℓ and ℓ' , and $K(\ell, \ell')$ is the force constant between two atoms located at sites ℓ and ℓ' . In our representation, the x and y axes are taken in the plane of the surface alloys, whereas the z axis is the outgoing normal to the surface plane of the x and y axes.

The application of Eq.(1) to an atom inside the Au crystal bulk gives a system of linear equations which may be cast in the following matrix form

$$D(\Omega) = \sum_{\varphi_x, \varphi_y} \sum_{p\alpha} \rho_{(\alpha, \alpha)}^{(p, p)}(\varphi_x, \varphi_y, \Omega) = - \frac{2\Omega}{\pi} \sum_{\varphi_x, \varphi_y} \sum_{p\alpha} \lim_{\epsilon \rightarrow 0^+} [Im G_{\alpha\alpha}^{pp}(\varphi_x, \varphi_y, \Omega + i\epsilon)] \quad (2)$$

The term $[\Omega^2 I - D(e^{\varphi_x}, e^{\varphi_y}, \mathcal{Z}, \lambda)]$ is the dynamics matrix, I denotes a unit matrix, \mathcal{Z} is a generalized phase factor between neighboring sites, λ is the ratio of the second neighbor to first neighbor force constants, k_2/k_1 , and \mathbf{U} is the displacements vector for the irreducible sites of the

basic unit cell in the crystalline bulk. $\Omega = \frac{\omega}{\omega_0}$ is a normalized frequency with respect to a characteristic frequency ω_0 of the bulk, where $\omega_0^2 = \frac{k_1}{M_{Au}}$.

The general solutions of Eq.(2) for the eigenmodes are calculated by requiring the determinant of the secular equation of the dynamic matrix to vanish. By diagonalizing the matrix of Eq.(2), for $Z = e^{i\varphi z}$, the phonon dispersion branches can be calculated along any direction in the lattice. For the Au crystalline bulk the secular equation may be expressed in general as a polynomial

$$\sum_s A_s Z^s = 0 \quad (3)$$

The coefficients A_s are functions of the dynamic variables $(\Omega, \varphi_x, \varphi_y)$, and of the elastic and structural properties of the system. Both the propagating and the evanescent eigenmodes may be calculated from Eq.(3), and are described by the phase factor doublets $\{Z, Z^{-1}\}$. Note that due to the hermitian nature of the dynamics, the phase factor doublets verify symmetrically the polynomial forms. The propagating phonon modes are determined consequently by the $|Z| = 1$ condition, and the evanescent modes by the $|Z| < 1$ condition. Eq.(3) is solved to yield the ensemble of propagating and evanescent modes $\{Z_j\}$ in the various frequency intervals of the bulk propagating bands. Only a part of these solutions are, however, of physical interest. For the propagating modes their inverses are phonon modes propagating in the opposite sense. For the non propagating modes only the evanescent modes $|Z| < 1$ are of physical interest.

The equations of motion for the atoms at the **Au(111) - ($\sqrt{3}x\sqrt{3}$)R30° - Pd** surface alloy may be written using Eq.(1). These are coupled to the rest of the semi-infinite Au crystal, generating a system of equations for which the number of unknown vibration displacements in the three regions defined by the matching theory, is greater than the number of equations. The resultant system of equations can be reduced by applying the matching formalism [34-37], leading to a finite square dynamic matrix. To do this, we need to describe the displacement vibration, for each set of dynamic variables $(\Omega, \varphi_x, \varphi_y)$, as a linear combination of the bulk eigenmodes, whether propagating or evanescent, along the direction normal to the surface going into the bulk crystal. In the modified representation, the vibration displacements of the intermediate and bulk sites are formally replaced thanks to the matching transformations. This procedure leads to a square dynamic matrix which characterizes a homogenous system of equations for which a non trivial solution permits the determination of localized eigenmodes at the boundary of the ordered surface alloy.

Furthermore, the local vibration densities of states (LDOS) in the ordered surface alloy **Au(111) - ($\sqrt{3}x\sqrt{3}$)R30° - Pd** can be calculated, per site and per atomic plane, by using the Green's function formalism. The Green's functions are calculated in a direct manner from the square matrix established by the matching formalism. The final expression of this LDOS is given by the following equation [39, 40]

$$D(\Omega) = \sum_{\varphi_y} \sum_{p\alpha} \rho_{(\alpha,\alpha)}^{(p,p)}(\varphi_y, \Omega) = -\frac{2\Omega}{\pi} \sum_{\varphi_y} \sum_{p\alpha} \lim_{\varepsilon \rightarrow 0^+} [Im G_{\alpha\beta}^{pp}(\varphi_y, \Omega + i\varepsilon)] \quad (4)$$

Using the matching theory we can also calculate the scattering of phonons at the surface alloy boundary. In this communication, however, we limit the presentation of our results to the vibration dynamics at the surface boundary.

4 Numerical results and discussion

4.1 $\text{Au}(111) - (\sqrt{3} \times \sqrt{3})R30^\circ - \text{Pd}$ surface phonons

In the present calculation we calculate the dynamic properties of the surface alloy $\text{Au}(111) - (\sqrt{3} \times \sqrt{3})R30^\circ - \text{Pd}$ system. In particular, we have calculated the surface phonons of the clean surface Au(111) as a reference system, in order to appreciate in contrast the effects of Pd atoms in the ordered surface alloy. The Au(111) surface presents a complex reconstruction [41], but the shift with respect to the ideal (111) surface is small enough to a first approximation to ignore the reconstruction for the surface lattice dynamics.

The linearized equations of motion governing the vibration displacements of atoms at different sites in the system, as in Eq.(1), are given in the harmonic approximation, which is valid for temperatures well below the solid liquid transition temperature of the two metallic materials, namely 1828 K for Pd and 1337 K for Au. In this approach the force constants for nearest and next nearest neighbors are sufficient to characterize the interaction potential. Other state of the art methods exist to calculate phonons, such as the *ab initio* methods, and it would indeed be useful to cross-check the results of the force field calculation presented in this paper with *ab initio* results when these are available.

The force constants between the first and second neighbors in the surface boundary of the system are given in our numerical calculations from Wu *et al* [42]. In this reference calculations are presented for transferable force constants as a function of the bond-length, for a variety of metal-metal interactions, including those for Au-Au and Au-Pd, using the Vienna *ab initio* simulation package which implements Bloch's projected augmented wave approach within the local density approximation. Given the crystalline structure at the surface boundary $\text{Au}(111) - (\sqrt{3} \times \sqrt{3})R30^\circ - \text{Pd}$, with no relaxation or reconstruction effects, we are able hence to determine numerical values for the required force constants for the intra- and inter-plane interactions. These are as follows, for Au-Au: $k_1 = 35.9 \text{ J/m}^2$ and $k_2 = 2.9 \text{ J/m}^2$, for Pd-Pd: $k_1 = 44.5 \text{ J/m}^2$ and $k_2 = 3.6 \text{ J/m}^2$, and for Au-Pd: $k_1 = 51.4 \text{ J/m}^2$ and $k_2 = 3.9 \text{ J/m}^2$. The atomic masses of Au and Pd are respectively $197.0u$ and $106.5u$.

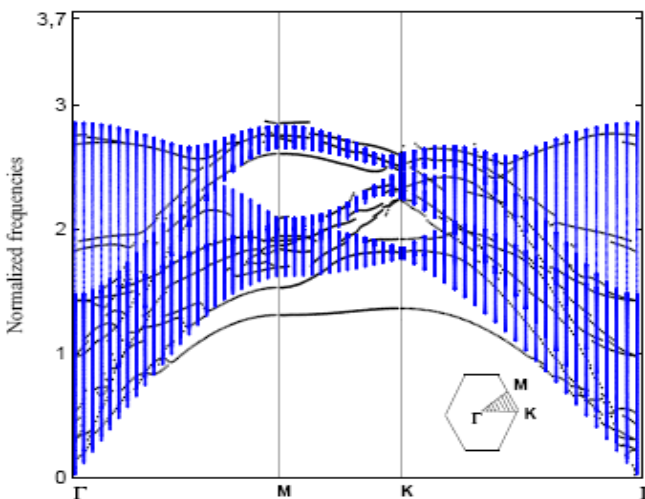


Fig.2. The calculated surface phonon dispersion curves and resonances (black curves) for the clean Au(111) surface

The calculated surface phonons for the clean surface Au (111) and the ordered surface alloy $\text{Au}(111) - (\sqrt{3} \times \sqrt{3})\text{R}30^\circ - \text{Pd}$, are given in general along the three directions of high symmetry $\overline{\Gamma\text{M}}$, $\overline{\text{MK}}$, and $\overline{\text{K}\Gamma}$ as shown in Figures. 2 and 3.

The results for the clean surface Au(111) in Figure 2, present two localised phonon branches beneath the bulk bands. The lowest one is the so-called Rayleigh branch. At long wave lengths (i.e. near the Γ point) this mode corresponds to essentially vertical deformation vibrations of the surface. At short wave lengths, however, its vibration character can change significantly, because it is more sensitive to short ranged interatomic couplings. This branch is comparable to that calculated previously by *ab initio* methods under the appellation S_1 [1]. Note that both sets of theoretical results, ours and those in reference [1], may be compared with the experimental data from [43]. Our results show a resonance branch in the first half of the interval $\overline{\Gamma\text{M}}$, near the lower limit of the bulk bands, which becomes a surface phonon branch in the second half of this interval, in agreement with the experimental data.

Our calculated results show another resonance in the interval $\overline{\text{K}\Gamma}$ near the lower limit of the bulk bands; in contrast this is a surface phonon branch in reference [1]. Again the experimental data are in agreement in part with our results, and in part with those of reference [1] for this branch. The other prominent features in Figure 2 are the calculated surface phonon branches at higher energies, located in the two energy gaps. These are also comparable to the branches S_2 and S_3 in reference [43], though displaced in our work to higher energies.

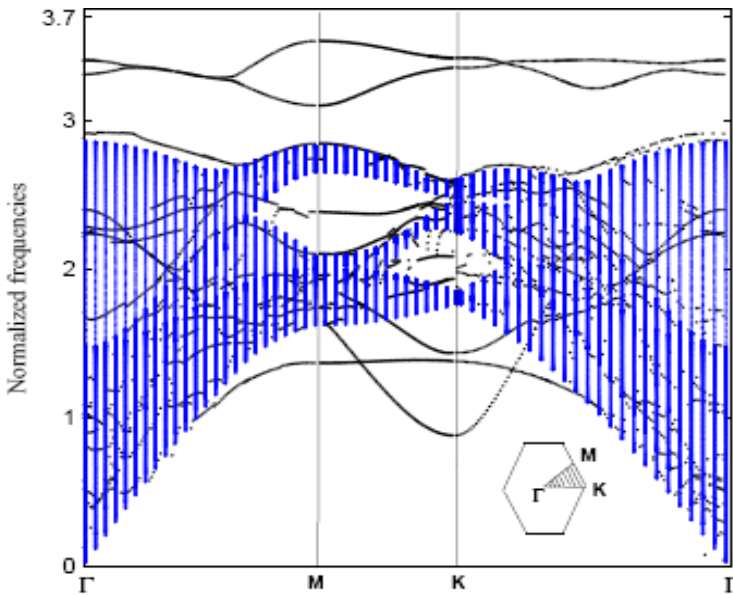


Fig. 3. The calculated surface phonon dispersion curves and resonances (black curves) for the $\text{Au}(111) - (\sqrt{3} \times \sqrt{3})\text{R}30^\circ - \text{Pd}$ surface alloy

In Figure 3, we present our calculations corresponding to the surface phonons of the ordered surface alloy $\text{Au}(111) - (\sqrt{3} \times \sqrt{3})\text{R}30^\circ - \text{Pd}$. The Rayleigh branch for the Au (111) surface is maintained and modified only very slightly for the surface alloy. However, two new branches appear beneath the bulk bands along the directions of high symmetry $\overline{\text{MK}}$ and $\overline{\Gamma\text{M}}$. Since there are no previous theoretical or experimental results to compare with, it is difficult to present any conclusions as regards these two branches at present. The branches in the two energy gaps are modified strongly by the presence of Pd in the topmost layer of the surface alloy. Given that the effective atomic mass

and elastic constants decrease and increase, respectively, in a mean field representation for the topmost layer, it is likely that the Au(111) branches are pushed higher up for the surface alloy **Au(111) – ($\sqrt{3}\times\sqrt{3}$)R30° – Pd**, to be replaced by resonances in the upper energy gaps.

Furthermore, the most striking feature in the phonon branches of the surface alloy in comparison with those of the clean Au(111) surface, is the appearance of new optic phonon branches. Indeed, the ordered **Au(111) – ($\sqrt{3}\times\sqrt{3}$)R30° – Pd** surface alloy exhibits three such surface phonons branches. One of them appears just at the upper limit of the bulk phonon bands. The two others appear high above the bulk bands. It is clear that the new branches are induced by the presence of the Pd monomers surrounded by six Au nearest neighbors in the topmost atomic layer. Since Pd is a lighter atom than Au yet connected by Au-Pd force constants superior to the individual Au-Au and Pd-Pd force constants, it is reasonable to expect the vibration LDOS to be highly concentrated on the Pd atom in the surface alloy. This is indeed the case as presented here after.

4.2 **Au(111) – ($\sqrt{3}\times\sqrt{3}$)R30° – Pd** surface vibration LDOS

The vibration local densities of states (LDOS) are calculated numerically per atomic site in the topmost surface layers, using a numerical procedure based in Eq.(4). The LDOS are given in arbitrary units, as a function of the normalized frequency Ω in the BZ. In Figure 4 we present the LDOS for the Au site in the topmost atomic layer of the clean Au(111) surface, this shall stand as a reference to compare with.

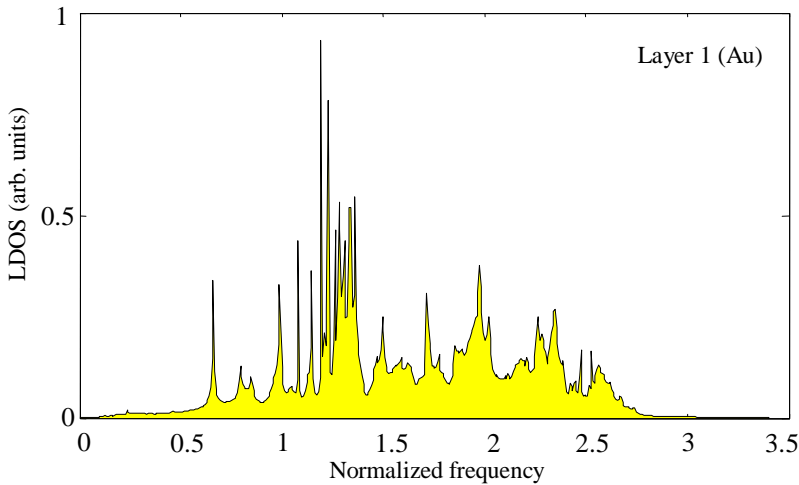


Fig.4. The local vibration density of states (LDOS) for the Au sites in the first atomic layer of the clean Au(111) surface.

In Figure 5, the LDOS for the Au and Pd sites in the topmost layer of the ordered surface alloy **Au(111) – ($\sqrt{3}\times\sqrt{3}$)R30° – Pd** are presented and identified as layer 1 (Au) and layer 1 (Pd), to distinguish them eventually from atomic Au sites in deeper layers. A general comparison between the LDOS for the Au and Pd sites in the surface alloy with that for the Au site on the clean Au(111) surface, shows important differences.

The first observation is that the surface alloy LDOS extends to higher energies. The second observation which we can note is the remarkable diminution of the LDOS for the layer 1 (Au) site spectrum on the surface alloy, in comparison with that for the layer 1 (Au) site in the clean Au(111) surface. Furthermore, the LDOS for the layer 1 (Pd) site in the surface alloy presents a remarkably

strong and widespread spectrum in comparison with that for the layer 1 (Au) site. Note in particular the increased DOS towards the higher energy limit for the layer 1 (Pd) site, which is completely absent from the Au (111) surface. These differences are certainly due to the presence of Pd atoms in the surface alloy, corresponding to a net transfer of vibrational activity from the Au sites to the Pd sites, reminiscent of the charge transfer from the Au to the Pd sites [24]. A deeper analysis of this point would need a clarification as to why the first neighbor alloy force constant $k_1(\text{Au-Pd})$ is greater than the individual $k_1(\text{Au-Au})$ and $k_1(\text{Pd-Pd})$ in the work of Wu et al. [42], and whether this is due to an effective charge transfer using their Vienna *ab initio* simulation package.

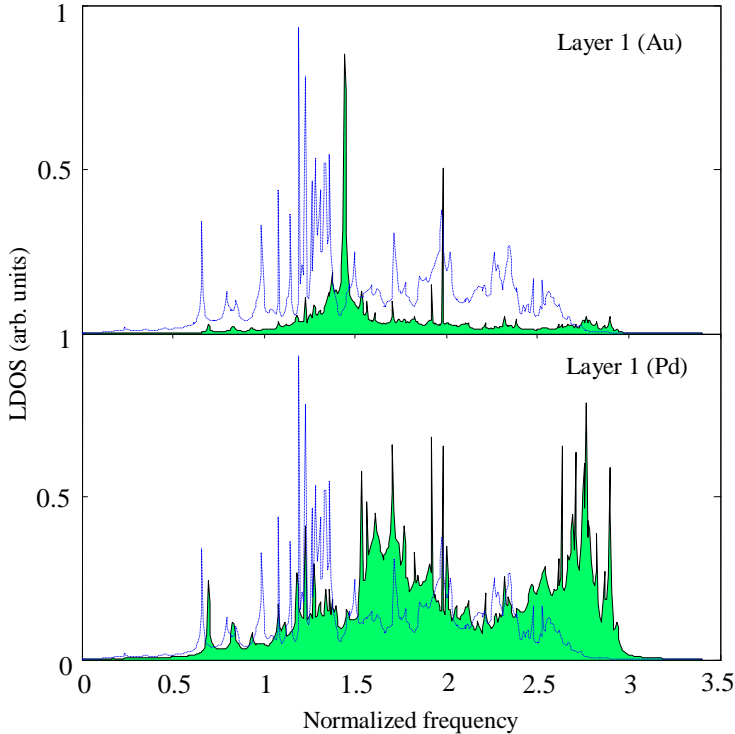


Fig.5. The local vibration densities of states (LDOS), for the Pd and Au sites in the 1st atomic layer of the **Au(111) - $(\sqrt{3}\times\sqrt{3})R30^\circ$ - Pd** ordered surface alloy. The reference discontinuous spectra is the LDOS for a site in the pure Au(111) surface.

In conclusion, this work reports a detailed investigation of the vibration and dynamic properties using the force field methods; in particular we calculate the surface phonons, resonances and vibration LDOS, for the Au(111) surface and for the **Au(111) - $(\sqrt{3}\times\sqrt{3})R30^\circ$ - Pd** surface alloy. The matching method used here proves to be an efficient theoretical tool for the analytical and numerical calculations. There are other methods to calculate surface phonons such as the *ab initio* methods, and it would indeed be useful to cross-check the results of the force field calculation presented in this paper with such results when these are available. One of these is the projector augmented plane wave method implemented in the VASP package. The PAW method is somewhat more accurate in describing the electronic structure than others at the expense of being a slower method. It is useful to note however that there is a trade-off in computational efficiency and predictive capability between *ab initio* and force field methods [44], the latter can also be more accurate than the former in certain cases.

References

1. R. Heid, and K.-P. Bohnen, editor: A.A. Maradudin, Phys. Reports **387**, 151 (2003)
2. D.S. Martin, N. P. Blanchard, and P. Weightman, Phys. Rev. B **69**, 113409 (2004)
3. A. de Siervo, E.A. Soares, R. Landers, T. A. Fazan, J. Morais, and G. G. Kleiman, Surf. Sci. **504**, 215 (2002)
4. M. Baldauf and D. M. Kolb, J. Phys. Chem. **100**, 11375 (1996)
5. A.M. El-Aziz, L.A. Kibler, J. Electroanalytical Chemistry **534**, 107 (2002)
6. B.E. Koel, A. Sellidj, and M.T. Paffett, Phys. Rev. B **46**, 7846 (1992)
7. P. J. Schäfer and L. A. Kibler, Phys. Chem. Chem. Phys. **12**, 15225 (2010)
8. D. Yuan, X. Gong, and R. Wu, Phys. Rev. B **75**, 085428 (2007)
9. D. Yuan, X. Gong, and R. Wu, Phys. Rev. B **78**, 035441 (2008)
10. B.S. Mun, C. Lee, V. Stamenkovic, N. M. Markovic, and P. N. Ross, Phys. Rev. B **71**, 115420 (2005)
11. J. Tang, M. Petri, L.A. Kibler, and D.M. Kolb, Electrochimica Acta **51**, 125 (2005)
12. C.-W. Yi, K. Luo, T. Wei, and D.W. Goodman, J. Phys. Chem. B **109**, 18535 (2005)
13. L.A. Kibler, M. Kleinert, R. Randler, and D. M. Kolb, Surf. Sci. **443**, 19 (1999)
14. Y. Ding, F. Fan, Z. Tian, and Z.L. Wang, J. Am. Chem. Soc. **132**, 12480 (2010)
15. T. Wei, J. Wang, and D.W. Goodman, J. Phys. Chem. C **111**, 8781 (2007)
16. B. Álvarez, V. Climent, J.M. Feliu, and A. Aldaz, Electrochemistry Comm. **2**, 427 (2000)
17. L.A. Kibler, A.M. El-Aziz, D.M. Kolb, J. Molecular Catalysis A: Chemical **199**, 57 (2003)
18. F. Calaza, F. Gao, Z. Li, and W.T. Tysoe, Surf. Sci. **601**, 714 (2007)
19. M.G. Vergniory, J.M. Pitarke, and S. Crampin, Phys. Rev. B **72**, 193401 (2005)
20. F. Reinert, G. Nicolay, S. Schmidt, D. Ehm, and S. Hüfner, Phys. Rev. B **63**, 115415 (2001)
21. A. Mugarza and J.E. Ortega, J. Phys.: Cond. Matter **15**, S3281 (2003)
22. T. Suzuki, Y. Hasegawa, Z.-Q. Li, K. Ohno, Y. Kawazoe, and T. Sakurai, Phys. Rev. B **64**, 081403 (2001)
23. I. Atanasov and M. Hou, Surf. Sci. **603**, 2639 (2009)
24. T. Eguchi, A. Kamoshida, M. Ono, M. Hamada, R. Shoda, T. Nishio, A. Harasawa, T. Okuda, T. Kinoshita, and Y. Hasegawa, Phys. Rev. B **74**, 073403 (2006)
25. S. Venkatachalam and T. Jacob, Phys. Chem. Chem. Phys. **11**, 3263 (2009)
26. H. Naohara, S. Ye, and K. Uosaki, J. Phys. Chem. B **102**, 4366 (1998)
27. A. Sellidj and B. E. Koel, Phys. Rev. B **49**, 8367 (1994)
28. C. J. Baddeley, C.J. Barnes, A. Wander, R.M. Ormerod, D. A. King, and R. M. Lambert, Surf. Sci. Lett. **314**, 1 (1994)
29. C. J. Baddeley, R.M. Ormerod, A.W. Stephenson, and R.M. Lambert, J. Phys. Chem. **99**, 5146 (1995)
30. M.S. Chen, K. Luo, T. Wei, Z. Yan, D. Kumar, C.-W. Yi, and D.W. Goodman, Catalysis Today **117**, 37 (2006)
31. L. Dobrzynski, J. Phys. Chem. Solids **30**, 1043 (1968); F. Garcia-Moliner and V. Velasco, *Theory of Single and Multiple Interfaces*, World Scientific (1992)
32. R. E. Allen, G.P. Alldredge, and F.W. de Wette, Phys. Rev. B **4**, 1648 (1971)
33. T. E. Feuchtwang, Phys. Rev. **155**, 731 (1967)
34. J. Szeftel and A. Khater, J. Phys. C: Solid St. Phys. **20**, 4725 (1987)
35. M. Belhadi, A. Khater, O. Rafil, and J. Hardy, phys. stat. sol. (b) **228**, 685 (2001)
36. A. Khater, M. Abou Ghantous, Surf. Sci. **498**, 97 (2002)
37. A. Khater, R. Tigrine, and B. Bourahla, phys. stat. sol. (b) **246**, 1614 (2009)
38. A. Maraudin, R. F. Wallis and L. Dobrzynski, *Handbook of Surfaces and Interfaces*, **3** Garland, New York (1980)
39. Niu-Niu. Chen and M. G. Cottam, Phys. Rev. B **44**, 14 (1991)
40. A. Virilouvet, H. Grimech, A. Khater, Y. Pennec, and K. Maschke, J. Phys: Cond. Matter **8**, 7589 (1996)
41. U. Harten, A.M. Lahee, J.P. Toennies, C. Wöll, Phys. Rev. Lett. **54**, 2619 (1985)

42. E. J. Wu, G. Ceder, and A. van de Walle, *Phys. Rev. B* **67**, 134103 (2003)
43. U. Harten, J.P. Toennies, Ch. Wöll, *Faraday Discuss. Chem. Soc.* **80**, 137 (1985)
44. E. Wimmer, *Mat. Sci.-Poland* **23**, 325 (2005)